

A Spitzer study of star-forming regions in Virgo Cluster galaxiesO. Ivy Wong¹, Jeffrey D. P. Kenney¹¹*Astronomy Department, Yale University, P.O. Box 208101 New Haven, CT 06520-8101*

ivy.wong@yale.edu

ABSTRACT

We present a preliminary study of the star formation distribution within three Virgo Cluster galaxies using the 24 μm Spitzer observations from the Spitzer Survey of Virgo (SPITSOV) in combination with $\text{H}\alpha$ observations. The purpose of our study is to explore the relationship between the star formation distribution within galaxies and the type (and phase) of interactions experienced within the cluster environment. Neither highly-obscured star formation nor strongly enhanced star-forming regions along the leading edges of galaxies experiencing ICM–ISM interactions were found. However, very unobscured star-forming regions were found in the outer parts of one galaxy (NGC 4402), while relatively obscured star-forming regions were found in the extraplanar regions of another galaxy (NGC 4522). We attribute the observed differences between NGC 4402 and NGC 4522 to the direction of motion of each galaxy through the ICM.

Subject headings: clusters: general — galaxy clusters: Virgo Cluster; individual (NGC 4522, NGC 4402, NGC 4501)

1. Introduction

Currently, the general understanding of galaxy evolution suggests that interactions play a significant role. However, the dominant processes are still not clear. Galaxy clusters provide a good laboratory in which to examine the effects of interactions on the evolution of individual galaxies within the cluster. The systematic differences in optical morphology between galaxies observed in the dense cores of clusters and those from the field regions (i.e. the morphology–density relation Dressler, 1980) suggest that galaxy evolution is strongly driven by the environment. Effects of the various forms of interactions have been observed

in detail in the Virgo Cluster where it is possible to spatially resolve regions of dust, gas and stars in individual galaxies.

Koopmann and Kenney (2004) used the spatial distribution of $H\alpha$ to study the environmental effects on star formation in the Virgo Cluster galaxies. However, $H\alpha$ observations are compromised by dust extinction effects. Without accounting for dust extinction effects, it is difficult to answer important questions about star formation such as: i) the existence of enhanced star-forming regions due to ram pressure or gravitational effects, and ii) the comparison between extraplanar and disk star formation rates. Recently, it has been shown that a combination of $H\alpha$ and $24\ \mu\text{m}$ emission has been found to be a reliable indicator of total star formation (Calzetti et al., 2007), since the $24\ \mu\text{m}$ emission is presumed to consist mostly of re-radiated dust emission from the extinguished star-forming regions. Hence, we intend to use a combination of $H\alpha$ and $24\ \mu\text{m}$ observations to explore how the type and phase of interaction experienced relates to the observed spatial variations of star formation within galaxies and the global variations between galaxies.

We present the preliminary study of three Virgo galaxies known to be three of the best examples of cluster galaxies experiencing ram pressure; NGC 4522, NGC 4402 and NGC 4501. Our preliminary study of these three galaxies is discussed in Section 2. Section 3 provides a summary.

2. Preliminary study on NGC 4522, NGC 4402 and NGC 4501

NGC 4522, NGC 4402 and NGC 4501 are three of the best examples of ram pressure stripping in action (Kenney, van Gorkom & Vollmer, 2004; Crowl et al., 2005; Vollmer et al., 2008, 2007). The HI deficiencies of these three galaxies indicate that these galaxies have approximately three to four times less HI as one would expect from a ‘normal’ galaxy. On the other hand, all three galaxies have very different gas truncation radii. NGC 4522 has a smaller gas truncation radius ($0.35\ R_{25}$; Kenney, van Gorkom & Vollmer, 2004) compared to that of NGC 4402 ($0.6\ R_{25}$; Crowl et al., 2005) because a significant amount of HI in NGC 4522 is extraplanar. And since NGC 4501 is still in a pre-peak phase of ram pressure stripping (Vollmer et al., 2008), its HI disk is truncated within the stellar disk ($\sim R_{25}$).

The effect of the ICM–galaxy interaction is best illustrated by comparing the optical stellar morphology to the HI or radio continuum morphology of each galaxy. As shown in Figure 1, the HI morphology of NGC 4522 is distorted and is shaped roughly like a bow-shock compared to the undisturbed stellar disk observed in the optical R -band (Kenney, van Gorkom & Vollmer, 2004). The HI morphology clearly shows the neutral gas

being stripped out of the disk as the galaxy travels through the ICM. Similarly, the radio continuum morphologies of NGC 4402 and NGC 4501 show compression on the sides of the leading edges as well as extended tails on the trailing sides (Crown et al., 2005; Vollmer et al., 2007, 2008). Evidence of compression and shear are also shown by the total polarization vectors (marked by the white vectors in Figure 1).

Figure 1 presents the $H\alpha$ and $24\ \mu\text{m}$ observations for NGC 4522 (column a), NGC 4402 (column b) and NGC 4501 (column c). Each column consists of five panels which (from top to bottom) show (i) the grayscale R -band image overlaid with the $H\text{I}$ or radio continuum contours as well as polarization vectors, (ii) the $H\alpha$ map, (iii) the $24\ \mu\text{m}$ map, (iv) the $H\alpha/24\ \mu\text{m}$ ratio map, and (v) the total star formation rate map determined from the observed $H\alpha+24\ \mu\text{m}$ emission.

Section 2.1 describes the star-forming regions and the total star formation rate observed in the three galaxies and the ratios of the $H\alpha$ to $24\ \mu\text{m}$ emission are discussed in Section 2.2.

2.1. Star formation in NGC 4522, NGC 4402 and NGC 4501

We aim to identify regions of ram pressure-induced star formation which might plausibly be occurring since all three galaxies show evidence of active pressure. Using the new $24\ \mu\text{m}$ data from the Spitzer Survey of Virgo (SPITSOV; see Kenney et al. in these proceedings) in combination with previous $H\alpha$ observations, we examine the total star formation rate within these galaxies. The total star formation rate can be derived using a linear combination of the observed $H\alpha$ and $24\ \mu\text{m}$ emission (Calzetti et al., 2007):

$$SFR(\text{M}_{\odot}\ \text{yr}^{-1}) = 5.3 \times 10^{-42} [L(H\alpha) + 0.031 L(24\mu\text{m})] \quad (1)$$

Estimates of the global star formation rates from the combination of $H\alpha$ and $24\ \mu\text{m}$ emission were found to be 1.5, 1.6 and 2.1 times that of the star formation rates derived from the $H\alpha$ emission alone (using the calibration from Kennicutt, 1998) for NGC 4501, NGC

Table 1: Total star formation rates of NGC 4402, NGC 4501 and NGC 4522.

Galaxy	Inclination	SFR	
		$H\alpha$	$H\alpha+24\ \mu\text{m}$
NGC 4402	80°	$0.28\ \text{M}_{\odot}$	$0.60\ \text{M}_{\odot}$
NGC 4501	62°	$1.67\ \text{M}_{\odot}$	$2.54\ \text{M}_{\odot}$
NGC 4522	79°	$0.10\ \text{M}_{\odot}$	$0.16\ \text{M}_{\odot}$

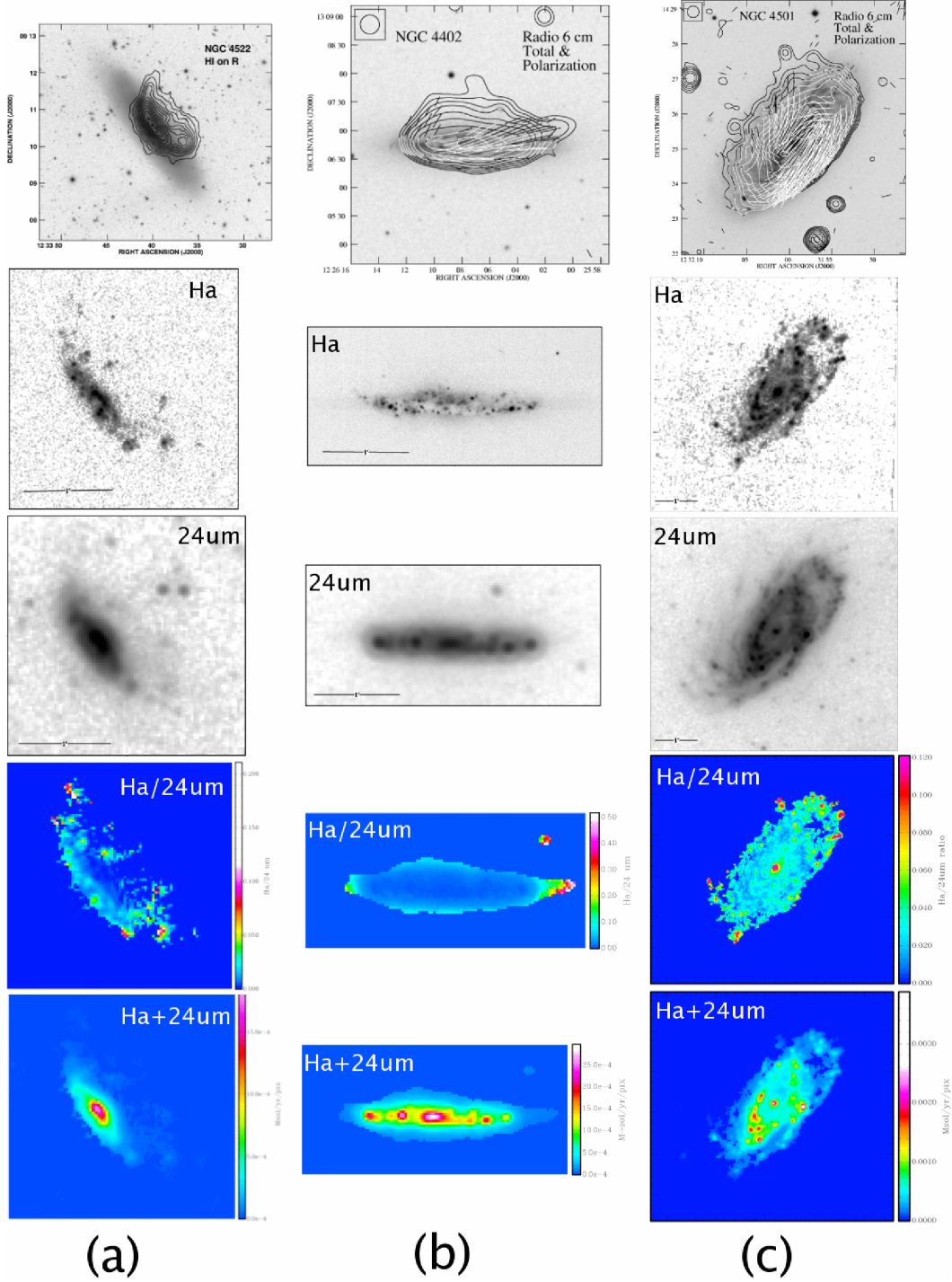


Fig. 1.— Columns (a), (b), (c) correspond to NGC 4522, NGC 4402 and NGC 4501, respectively. Each columns consists of 5 panels; which show (from top to bottom) the grayscale R -band image overlaid with HI or radio continuum contours as well as polarization vectors, the $H\alpha$ image, the $24\mu\text{m}$ image, the $H\alpha+24\mu\text{m}$ star formation map and the $H\alpha/24\mu\text{m}$ ratio map.

4522 and NGC 4402, respectively (see Table 1). The greatest difference is observed in the most inclined galaxy ($i = 80^\circ$), NGC 4402. Therefore, the difference between the total star formation rates derived using the two methods appears to be correlated with the observed inclination of the galaxy. This suggests that more inclined galaxies with more dust will have a greater $24\ \mu\text{m}$ contribution to the total star formation rate.

From the total star formation rate maps of all three galaxies (in Figure 1), the regions of most intense star formation are found in the galaxy centers and inner disk regions. We do not find any strongly-enhanced star-forming regions along the leading edges of interaction. However, extraplanar star formation is clearly observed in NGC 4522 where stars have been formed from the stripped gas and are entering the galaxy halo or intracluster space. By comparing the $\text{H}\alpha$ and $24\ \mu\text{m}$ fluxes in the disk and extraplanar regions of NGC 4522, we find that $\sim 18\%$ of the total $24\ \mu\text{m}$ flux and $\sim 11\%$ of the total $\text{H}\alpha$ emission originated from the extraplanar regions of NGC 4522. This implies that the extraplanar star-forming regions are more obscured, on average, than the disk regions. It is possible that the dust is being pushed between the observer and the star-forming regions as NGC 4522 travels away from the observer through the ICM.

2.2. Spatial distribution of $\text{H}\alpha$ to $24\ \mu\text{m}$ emission ratios

For a galaxy moving towards the observer, one might expect ram pressure to sweep the dust behind the observed star-forming regions causing a lower $\text{H}\alpha$ attenuation. Conversely, a galaxy moving away from the observer may display a higher $\text{H}\alpha$ attenuation as more stripped dust is pushed between the observer and the star-forming regions. Using the $\text{H}\alpha/24\ \mu\text{m}$ ratios, we investigate the spatial distribution of $\text{H}\alpha$ attenuation in our sample of cluster galaxies where ram pressure is active. It should be noted that both NGC 4501 and NGC 4522 are moving away from the observer, while NGC 4402 is moving towards the observer.

As expected, the most obscured regions of star formation are found in the galaxy centers (see the $\text{H}\alpha/24\ \mu\text{m}$ ratio maps in Figure 1), whereas the least obscured star-forming regions are found in the outer edges of all three galaxies. In particular, regions of high $\text{H}\alpha/24\ \mu\text{m}$ ratios are observed (from Figure 1) near the leading edge of interaction of NGC 4522.

The global $\text{H}\alpha/24\ \mu\text{m}$ ratios of our three galaxies are smaller than the median $\text{H}\alpha/24\ \mu\text{m}$ ratio (0.034) of the SINGS sample used by Calzetti et al. (2007). We find $\text{H}\alpha/24\ \mu\text{m}$ ratios of 0.029, 0.023 and 0.008 for NGC 4501, NGC 4522 and NGC 4402, respectively. It should be noted that the SINGS sample used by Calzetti et al. (2007) consists of galaxies spanning the full range of inclinations, while our galaxies have inclinations ranging from

62° to 80°. Our current results suggest that a greater inclination may be correlated with a smaller global $H\alpha/24\ \mu\text{m}$ ratio.

Recently, Prescott et al. (2007) found decreasing radial trends in $H\alpha$ attenuation by dust for a majority of the SINGS galaxies. Similar to Prescott et al. (2007), we selected regions with circular apertures of 500 pc and measured the ratios of $\nu L_\nu(24)/L(H\alpha)$ as a function of the projected radius from the centers of our galaxies. However unlike Prescott et al. (2007), our regions were selected from the $H\alpha$ observations as well as the 24 μm observations in order to probe the outer star-forming regions more effectively and avoid biasing against very unobscured regions. Although an aperture size of 500 pc is not optimal for separating individual star-forming regions, it is comparable to the spatial resolution of the 24 μm observations.

Figures 2, 3 and 4 show the regions selected in NGC 4522, NGC 4402 and NGC 4501, respectively. The first two panels of each figure (from the left) show the $H\alpha$ and the 24 μm map of the galaxy with the selected regions overlaid. The final panel of each figure (c) plots $\nu L_\nu(24)/L(H\alpha)$ as a function of projected radius from the galaxy center. The selected regions are loosely divided into three categories; regions on the side of the leading edge (red), extraplanar or outer disk regions (blue) and regions in the inner disk (green). These categories are color-coded for easier identification and the color of the apertures shown on the maps correspond directly to the color of the dots on the plot in panel (c).

The average 24 $\mu\text{m}/H\alpha$ ratios measured from the inner disk regions (green regions) of the three galaxies are greater than those measured from the outer disk or extraplanar regions (blue regions). The average ratios for the inner disk regions of all three galaxies are very similar (with values between 2.52 and 2.64) but the difference in the 24 $\mu\text{m}/H\alpha$ ratio between the inner and outer regions varies significantly for each galaxy. The minimum difference in average ratios between the inner and outer disk is $\sim 1.6\%$ for NGC 4501 and the maximum difference between the outer and inner disk is $\sim 22.9\%$ for NGC 4402. Since NGC 4402 is highly inclined, the 24 μm observations will be biased by the dusty disk of the galaxy. However, the motion of NGC 4402 towards the observer is able to push the dust from the outer disk (or extraplanar) regions behind star-forming regions as these regions are not as affected by the dusty center. This may explain the fact that a decrease in the 24 $\mu\text{m}/H\alpha$ ratio is observed only at the two extreme ends and the extraplanar HII region of NGC 4402.

Of the three galaxies analysed, NGC 4402 exhibits the most convincing radial decrease in the 24 $\mu\text{m}/H\alpha$ ratio (see Figure 3). Its 24 $\mu\text{m}/H\alpha$ ratio is highest in the central 0.5 kpc and then decreases very gradually to 4 kpc. The two outer disk regions on both sides of the disk (as represented by the two blue points at radius $\sim 4\text{--}5$ kpc in panel (c) of Figure 3) exhibit a clear decrease in the 24 $\mu\text{m}/H\alpha$ ratios. In addition, the region at the largest

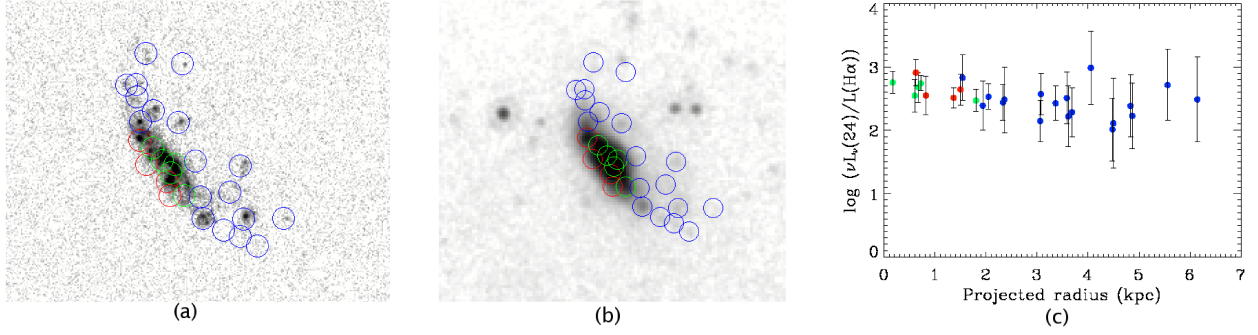


Fig. 2.— The 24 $\mu\text{m}/\text{H}\alpha$ ratio of 500 pc regions in NGC 4522. The H α and 24 μm observations overlaid with regions of 500 pc diameter apertures are shown in panels (a) and (b), respectively. The regions are divided into three categories; regions within the inner disk (green), regions on the leading edge of the ISM–ICM interaction (red) and outer disk or extraplanar regions (blue). Panel (c) shows the 24 $\mu\text{m}/\text{H}\alpha$ ratio of each 500 pc region as a function of the projected radius from the center of the galaxy. The regions circled in blue, red and green correspond to the blue, red and green dots in the right panel respectively.

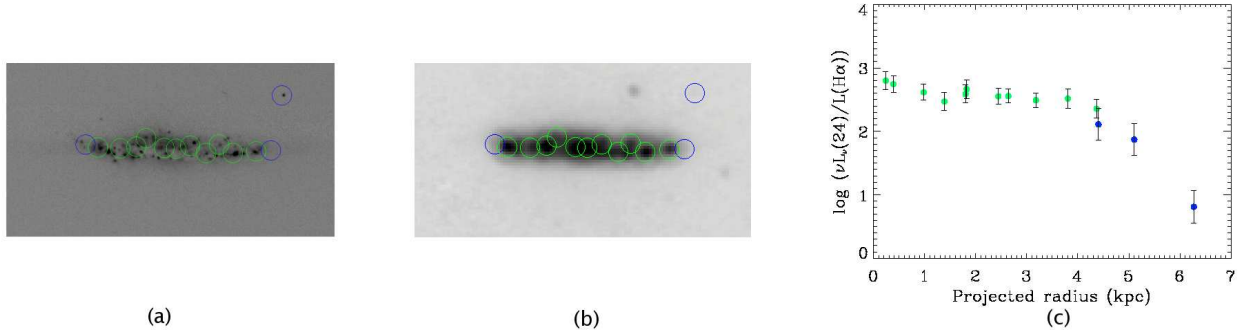


Fig. 3.— The 24 $\mu\text{m}/\text{H}\alpha$ ratio of 500 pc regions in NGC 4402. See figure 2 for more details.

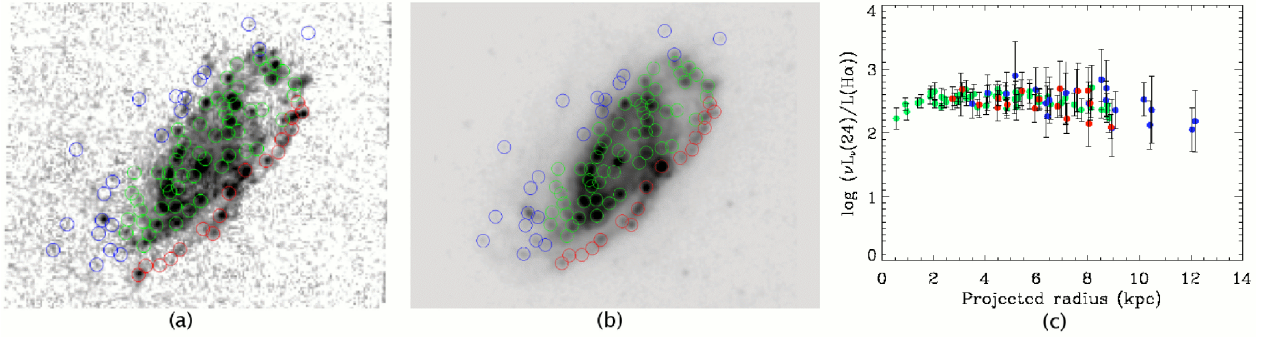


Fig. 4.— The 24 $\mu\text{m}/\text{H}\alpha$ ratio of 500 pc regions in NGC 4501. See figure 2 for more details.

projected radius is an HII region, *122603+130724*, which appears to be the *most unobscured* star-forming region found in the current analysis. This extraplanar HII region is thought to have formed from enriched material stripped from NGC 4402 (Cortese et al., 2004). It should be noted that these three outermost regions in NGC 4402 have fairly low $H\alpha$ luminosities (i.e. they are not high luminosity HII regions with low obscuration).

Even though bright star-forming regions have been observed near the leading edge in the optical images of NGC 4402 (Crowl et al., 2005), the $24\ \mu\text{m}/H\alpha$ ratios in this part of the galaxy do not appear unusual. The $24\ \mu\text{m}/H\alpha$ ratios of NGC 4402 are comparable to the ratios obtained by Prescott et al. (2007) for the highly-inclined SINGS sample. The lowest $\log [\nu L_\nu(24)/L(H\alpha)]$ ratio found by Prescott et al. (2007) for the highly-inclined SINGS sample is ~ 0.6 , while the most unobscured extraplanar HII region in NGC 4402 is ~ 0.8 . On scales of 500 pc, it is not possible to identify leading edge regions in this galaxy due to resolution constraints.

Unlike NGC 4402, we do not find significant radial decreases in the $H\alpha$ attenuation for NGC 4501 and NGC 4522. A very slight radial decrease in the $H\alpha$ attenuation is observed in NGC 4522 (Figure 2) but there remains a large scatter in the ratios measured from the outer disk (or extraplanar) regions. Unlike Figure 1, we do not find any evidence for highly-unobscured star formation along the leading edge of NGC 4522 in Figure 2. This may be due to the fact that the regions of low $H\alpha$ attenuation in NGC 4522 are located in small regions with low luminosities. Consequently, the effect of decreased $H\alpha$ attenuation from these regions is diminished when the ratios are averaged across 500 pc apertures. In addition, the obscuration of the extraplanar regions of this galaxy is enhanced due to its direction of motion away from the observer through the ICM.

Similar to NGC 4522, only a slight decrease is found in NGC 4501 (Figure 4). There are two possible explanations which may account for the lack of an observed decrease in the $H\alpha$ attenuation at the leading edge. Firstly, NGC 4501 is travelling through the ICM away from the observer which will result in a displacement of the gas and dust from the regions close to the leading edge towards the observer. Secondly, Vollmer et al. (2008) concluded that NGC 4501 is in a pre-peak stripping stage and that ram pressure will only reach its maximum in ~ 100 Myr. Hence, it is possible that the current ram pressure is not strong enough to remove enough dust at the leading edge even though there is enough pressure to strip off the diffuse gas.

3. Summary

Using the 24 μm observations obtained from the Spitzer Survey of Virgo (SPITSOV) in combination with $\text{H}\alpha$ observations, we explored the distribution of star-forming regions within three Virgo Cluster galaxies (NGC 4402, NGC 4501 and NGC 4522) which are experiencing active ram pressure. The combination of the 24 μm and $\text{H}\alpha$ observations allowed us to uncover regions of significant dust obscuration. From this we are able to produce total star formation maps without the usual bias caused by dust extinction.

From our preliminary analysis of NGC 4522, NGC 4402 and NGC 4501, we find evidence neither for highly obscured star forming regions nor for strongly enhanced star formation along the leading edges of interaction. The $\text{H}\alpha$ attenuation (ratio between $\text{H}\alpha$ and 24 μm emission) of these three galaxies are comparable to the non-cluster SINGS galaxies studied by Calzetti et al. (2007) and Prescott et al. (2007). However, NGC 4402 exhibits unobscured outer disk and extraplanar star-forming regions, while, the outer disk and extraplanar star-forming regions of NGC 4522 appears moderately obscured. We attribute the differences between these two galaxies to the direction of motion of each galaxy through the ICM.

This work is based on observations made with the Spitzer Space Telescope, which is operated by the Jet Propulsion Laboratory, California Institute of Technology under a contract with NASA. Support for this work was provided by NASA through an award issued by JPL/Caltech.

REFERENCES

- Calzetti, D. et al. 2007, ApJ, 666, 870
- Cortese, L., Gavazzi, G., Boselli, A. & Iglesias-Paramo, J. 2004, A&A, 416, 119
- Crowl, H.H., Kenney, J.D.P., van Gorkom, J.H. & Vollmer, B. 2005, AJ, 130, 65
- Dressler, A. 1980, ApJ, 236, 351
- Kenney, J.D.P., van Gorkom, J.H. & Vollmer, B. 2004, AJ, 127, 3361
- Kennicutt, R.C., Jr. 1998, ARA&A, 36, 189
- Koopmann, R.A. & Kenney, J.D.P. 2004, ApJ, 613, 866
- Prescott, M.K.M., et al. 2007, ApJ, 668, 182

Vollmer, B., et al. 2007, A&A, 464, 37

Vollmer, B., et al. 2008, A&A, *in press*